

Enhancement and suppression of shot noise in capacitively coupled metallic double dots

M. Gattobigio,*

Scuola Normale Superiore, Piazza dei Cavalieri, 7, I-56126 Pisa, Italy

G. Iannaccone and M. Macucci

Dipartimento di Ingegneria dell'Informazione, Università degli Studi di Pisa, via Diotisalvi 2, I-56122 Pisa, Italy

(Received 13 September 2001; published 8 March 2002)

We present the peculiar noise behavior of bistable systems of coupled quantum dots during switching between the two stable states. Shot noise of the current through different branches of the system can be suppressed and/or enhanced up to a few times the “full” shot-noise level. Results from Monte Carlo simulations and from an analytical model are presented.

DOI: 10.1103/PhysRevB.65.115337

PACS number(s): 73.23.Hk, 72.70.+m, 73.63.Kv

I. INTRODUCTION

In the investigation of transport mechanisms in nanostructured devices, modeling and measurement of shot noise, i.e., nonequilibrium current fluctuations associated with the granularity of charge, could provide additional information not otherwise available through dc transport analysis.

Poisson statistics describes electron motion when there is no correlation between electrons. In this case the “full” shot noise is observed and the zero-frequency power spectral density is $S_P(0) = 2qI$,¹ where q is the electron charge and I is the average current. Deviations from this behavior are due to the presence of correlation between charge carriers. There are mainly two kinds of correlation. First, there are correlations due to the Pauli exclusion principle, which cause reduction of shot noise with respect to the “full shot” level. It is known, for instance, that in quantum point contacts shot noise is totally suppressed in conductance plateaus. Instead, in diffusive conductors the suppression is 1/3 with respect to the full shot-noise level (for a thorough review of experimental and theoretical investigations see Ref. 2). A second source of correlation is Coulomb interaction. This is extremely important in Single Electron Tunneling (SET) devices, in which the very nature of the transport mechanism is associated with Coulomb interaction, which in metal quantum dots is taken into account through the charging energy of tunneling junctions.

The theory of shot noise in SET's has been developed by Hershfield *et al.*,³ for one of the simplest SET devices, consisting of two double junctions connected in series. They demonstrate, for instance, that in the Coulomb staircase regime, i.e., for strongly asymmetric junctions, shot noise can be suppressed down to 1/2 of the full shot level. Experimental evidences of this behavior have been shown by Birk *et al.*⁴ In addition, other authors have shown, both theoretically⁵ and experimentally,⁶ the possibility of an even greater suppression in the regime of Coulomb oscillations, when the number of electrons in the dot is driven by an external gate.

Recently, shot noise in SET devices such as arrays of tunnel barriers has been studied in order to better understand the conditions under which transport can be considered as a discrete or a quasicontinuous charge transfer.^{7–9}

In all of the above examples, negative correlation of the electron motion leads to suppression of shot noise.

In this paper we will also report an example of shot-noise enhancement due to a positive correlation between electron tunneling events. There are few situations in which this behavior has been investigated. Mainly, shot-noise enhancement has been studied in double-barrier resonant diodes,^{10–15} in which the mechanism leading to a super-Poissonian shot noise is the existence of a negative differential conductance region in the current–voltage characteristic.

Shot-noise enhancement has been also theoretically predicted in a single tunneling barrier,^{16,17} in which the space-charge region preceding the barrier controls the tunneling transmission probability.

In this paper we investigate the shot-noise behavior in a SET device made up of two capacitively coupled metallic double dots (CMDD). In Fig. 1 we report an equivalent circuit diagram for this structure. Tunneling is allowed between the dots forming each double-dot structure, for instance, between dots 1 and 2, between dots 3 and 4, and between the dots and the external leads. This allows current to flow be-

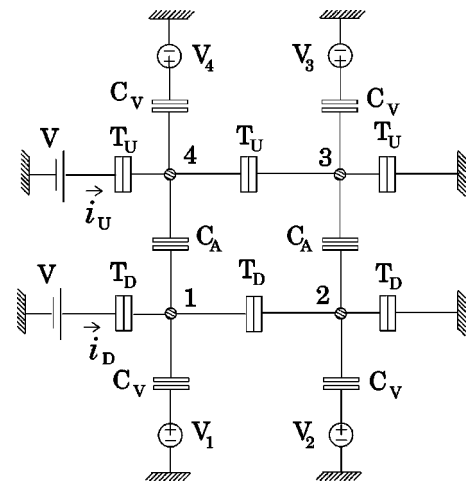


FIG. 1. Equivalent circuit of the CMDD. Tunneling junctions are represented by tunneling capacitors, (as, for example, the one between dots 1 and 2), while electrostatic interaction between the upper and the lower pair of dots, and between dots and gates is represented by classical capacitors.

tween two leads through dots 1 and 2 (current i_D), and through dots 3 and 4 (current i_U) once a small voltage difference is applied between the right and left leads. We are interested in the case in which an excess electron is present in each double dot. Due to the electrostatic repulsion, at the equilibrium, the two electrons occupy antipodal dots (1 and 3 or 2 and 4). If the chemical potentials values in the dots forming a double-dot structure are not aligned, there is no current flow and, therefore, we are in the Coulomb-blockade regime. Using the bias on the external gates to align the chemical potential values in the dots with those in the leads, we can bring the system out of the Coulomb-blockade regime, and current will flow through the pair of dots.

We study shot noise in currents i_D and i_U in this situation. We will show the peculiar behavior of shot noise when a pair of dots, for instance, the upper one, is in the conducting regime while the other is on the edge of Coulomb blockade. In this case the current i_U shows the typical suppression of shot noise, while the current i_D shows a strong shot-noise enhancement. From a qualitative point view, this behavior is due to the strong correlation between transitions of electrons from dot 4 to dot 3 and from dot 2 to dot 1: an electron tunneling from dot 4 to dot 3 *pushes* an electron from dot 2 to dot 1, and, until the electron remains on dot 2, further tunneling from dot 4 to 3 is suppressed; then, when the electron transition from dot 2 to dot 1 occurs, tunneling from dot 4 to 3 is enabled again, but further tunneling from dot 2 to 1 is suppressed until the transition from dot 4 to 3 occurs. Since the lower pair of dots is on the edge of Coulomb blockade, the characteristic time of transitions from dot 2 to 1 is much larger than the characteristic time of transitions from dot 4 to 3. For this reason, this mechanism introduces negative correlation between current pulses in i_U (i.e., “regulates” the sequence of current pulses) and, therefore, suppressed shot noise, while introduces positive correlation between the current pulses in i_D , and, therefore, enhanced shot noise. We will analyze this mechanism in detail in the following sections.

The paper is organized as follows: in Sec. II we describe the circuit representation of the CMDD that we have considered in our simulations. We briefly describe the Monte Carlo algorithm that we have implemented and the estimator we have used for the Fano factor γ , i.e., the ratio, at zero frequency, of the noise power spectrum to the full shot-noise power spectrum. In Sec. III we report the numerical results, beginning with the investigation of shot noise in a single double-dot structure, also known as single-electron pump,^{18,19} and then proceeding with the discussion of the results we have obtained in CMDD. In Sec. IV we describe an analytical model, based on a formalism borrowed from Ref. 20, developed in order to clarify the mechanism that is responsible for the peculiar shot-noise behavior, at low temperature. The analytical results are compared with the numerical ones and good agreement is obtained. Finally, Sec. V contains some concluding remarks.

II. FORMALISM

In order to evaluate the shot noise of the currents that flow through the CMDD system, we have developed a Monte

Carlo code based on the semiclassical theory of the Coulomb Blockade.²¹ In the following we will describe the model we have used for the CMDD, based on classical and tunneling capacitors, and the expressions for the calculation of the Fano factor.

A. Circuitual representation of CMDD

The metal-island system reported in Fig. 1 has been proposed as the elementary cell of the Quantum Cellular Automaton (QCA) architecture.²² Indeed, using two excess electrons, two logical states can be encoded in this structure, and properly structured two-dimensional arrays of such cells can implement any logical function.

While QCA architectures have several interesting features and intrinsic advantages with respect to conventional complementary metal-oxide conductor architectures, fundamental and technological problems have been assessed that prevent any practical implementation of large-scale circuits, at least with solid-state technology.^{23,24} However, the QCA architecture is beyond the scope of this paper, and we consider the circuit shown in Fig. 1 as a testbed for investigating noise properties in SET circuits.

Tunneling between adjacent dots and between dots and external leads is taken into account by means of tunneling capacitors. A tunneling capacitor is characterized by a capacitance C , and by a resistance R , which enters the orthodox formula of the tunneling rate²¹

$$\Gamma = \frac{1}{e^2 R} \frac{\Delta E}{1 - \exp(-\Delta E/k_B T)}, \quad (1)$$

where e is the electron charge, k_B the Boltzmann constant, T the temperature, and ΔE is the free-energy variation. We have used the following expression in order to evaluate it:

$$\Delta E = \delta \left(\frac{1}{2} \sum_{i,j \in \text{islands}} (q_i + \tilde{q}_i) C_{ij}^{-1} (q_j + \tilde{q}_j) \right) + \sum_{k \in \text{sources}} V_k \delta q_k, \quad (2)$$

where q_i is the charge in the i th dot, C^{-1} is the inverse capacitance matrix, and \tilde{q}_i is the charge bias induced by the coupling between the i th dot and external voltage sources, and it is defined as $\tilde{q}_i = \sum_{k \in \text{sources}} C_k V_k$. The summation is only performed over voltage sources V_k connected to the i th dot via a capacitance C_k . The last term in Eq. (2) represents the work done by the source V_k if the tunneling of a charge δq_k occurs through a junction connecting the source with the dot.

We denote the circuit elements in the upper section with the subscript U : we have tunneling capacitors T_U with capacitance C_U and resistance R_U . Circuit elements in the lower section have completely analogous denominations, except for the subscript, which is D for this latter case. Interaction between the two pairs of dots is introduced by means of the capacitors C_A . Finally, C_V represents the capacitive coupling with the external gates. In our simulation we have

used the following numerical values: $C_U=0.5$ aF, $C_D=0.5$ aF, $C_A=1.2$ aF, $C_V=0.42$ aF, $R_D=R_U=5$ M Ω , and $V=2$ mV. We note that the values of tunneling resistances are much larger than the resistance quantum $R_q=h/2e^2\approx 12.9$ k Ω , as required by the orthodox theory in order to ensure electron localization.

For each given configuration of gate voltages, the time evolution is computed in the following way. The free-energy variations ΔE associated with all possible transitions of a single electron through a junction are evaluated and the related probability rates are obtained from Eq. (1). A transition is then chosen at random, according to such probabilities, and the charge configuration is updated. Then the time interval between this and the following transition is generated as an exponentially distributed random number with average equal to the inverse of the total tunneling rate, obtained as the sum of the rates for all possible transitions. The evolution stops when a given observation time \mathcal{T} is reached. For each voltage configuration, a few thousands of time histories are generated in order to obtain a large ensemble on which we perform the averages required for shot-noise evaluation.

B. Power spectral density and cross-correlation estimator

The power spectral density of a real random process $i(t)$ is defined as the Fourier transform of the correlation function

$$S(\omega) = 2 \int_{-\infty}^{\infty} dt e^{-i\omega t} [\overline{i(t)i(0)} - I^2]. \quad (3)$$

In Eq. (3) we have used the overline notation to denote *ensemble* averages and $I \equiv \overline{i(t)}$.

We are dealing with a finite process, then we need an estimator of Eq. (3). Let \mathcal{T} be the time of observation, then a good estimator is

$$P_{\mathcal{T}}(\omega) = \frac{2}{\mathcal{T}} \left| \int_0^{\mathcal{T}} dt e^{-i\omega t} [i(t) - I] \right|^2. \quad (4)$$

Indeed, if we evaluate its expectation value we get,

$$S_{\mathcal{T}}(\omega) \equiv \overline{P_{\mathcal{T}}(\omega)} \approx S(\omega) + \frac{1}{2\pi^2\mathcal{T}^2} \frac{d^2 S}{d\omega^2}(\omega) \int_{-1}^1 \frac{dx}{\pi} x^2 \left(\frac{\sin x}{x} \right)^2, \quad (5)$$

where we have neglected terms of order $o(1/\mathcal{T}^4)$. Letting \mathcal{T} go to infinity, we recover the power spectral density

$$\lim_{\mathcal{T} \rightarrow \infty} S_{\mathcal{T}}(\omega) = S(\omega). \quad (6)$$

In our model the random process is the current that flows through the external voltage source when an electron tunneling event occurs. The expression of this current is

$$i(t) = \sum_{0 \leq t_k \leq \mathcal{T}} \delta q_k \delta(t - t_k), \quad (7)$$

where δq_k is the charge flowing through the voltage source at the tunneling event time t_k . The pulse shape can be described as a δ function because we are interested only in

low-frequency noise. Using Eq. (7) and $S_{\mathcal{T}}$ for the estimation of the spectral density we get the following expression of the Fano factor γ :

$$\gamma \equiv \frac{S(0)}{2e\overline{i(t)}} = \frac{\overline{\sum_{k,j} \delta q_k \delta q_j - \sum_k \delta q_k^2}}{e \sum_k \delta q_k}. \quad (8)$$

We collect a few thousand time evolutions, each of them lasting a time \mathcal{T} . Such a collection is used to evaluate the averages in Eq. (8) and, therefore, to calculate the Fano factor.

We are also interested in the cross correlation between the upper and the lower current. Following the same steps as for the spectral density case, we get the following estimator for the cross-correlation factor at zero frequency:

$$C = \frac{\overline{\sum_{k,j} \delta q_k^U \delta q_j^D - \sum_k \delta q_k^U \sum_k \delta q_k^D}}{\sqrt{\gamma^U \gamma^D \sum_k \delta q_k^U \sum_k \delta q_k^D}}, \quad (9)$$

where we use superscript D for the lower circuit quantities, and U for the upper circuit quantities.

III. NUMERICAL RESULTS

A. Single-electron pump

We start our numerical analysis of shot noise from the case in which there is no interaction between the upper and the lower pair of dots. Let us focus only on the lower pair of Fig. 1. We are dealing with a device known as *single-electron pump*:²⁵ at zero-bias voltage, i.e., $V=0$, the stable configurations of the device tile the plane ($\tilde{Q}_1 \equiv V_1 C_V$, $\tilde{Q}_2 \equiv V_2 C_V$) with elongated hexagons, yielding the so called honeycomb diagram. Let us define the points at the intersection of three different stable configurations *triple points*. When a bias V is applied, the previous honeycomb structure is distorted, and the triple points become wider regions of instability between the different stable charge configurations. If we consider the current flowing in the pair, we find, as it is well known, that in correspondence with the triple points there are current peaks.^{18,19}

The operation of a single-electron pump consists in placing the circuit configuration in the vicinity of a triple point. Then two periodic signals with the same frequency but a phase difference of $\pi/2$ are applied to V_1 and V_2 , in order to follow a closed path in the configuration space all around the triple point. When a closed path is completed, an electron has been moved from one external lead to the other. We have evaluated the Fano factor of current i_D as a function of V_1 and V_2 , and the result is reported in Fig. 2. In this device we have only suppression of shot noise. Dark regions of Fig. 2 correspond to $\gamma \approx 1$, bright regions to smaller γ . As can be seen, the Fano factor reproduces the honeycomb structure. The larger i_D , the smaller the Fano factor γ . At the triple point the Fano factor reaches its minimum value of $1/3$.²⁶

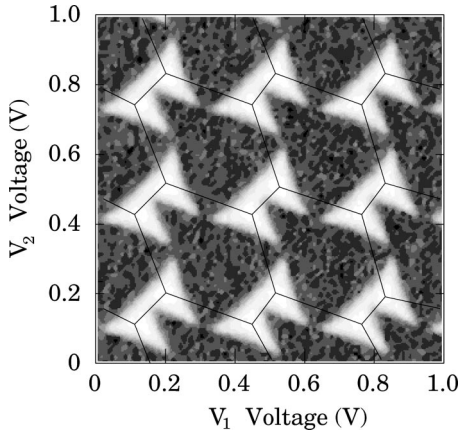


FIG. 2. Fano factor γ of a single-electron pump at the temperature of 20 K. Dark regions correspond to $\gamma \approx 1$ and bright regions to smaller γ .

B. Shot noise in a CMDD structure

Let us proceed with a discussion of the results of the numerical simulations in the CMDD structure, which is an interacting couple of single-electron pumps.

In the Introduction we have anticipated how the CMDD is operated in our investigation of shot-noise behavior. With reference to Fig. 1 for the symbols, a small voltage V is applied to the external leads in order to have currents i_U and i_D flowing in the upper and in the lower pair of dots, respectively, whenever the chemical potentials in the corresponding single-electron pump are aligned. If there is no alignment, no current flows through the leads, and the system is in the Coulomb-blockade regime.

The chemical potential of the n th dot is mainly influenced by the external gate V_n . Let us describe how to align the chemical potential of two dots, for instance, dots 1 and 2: we apply a voltage ramp with a negative slope to dot 1, in our example $V_1 = 0.88 \text{ V} - V_D$, where V_D varies linearly in time in the range between 0 V and 0.6 V, as reported in Fig. 3. We also apply a voltage ramp with positive slope to dot 2, $V_2 = -0.48 \text{ V} + V_D$. In this way, we allow the chemical potential values on dots 1 and 2 to align, at some specific time, with the Fermi energy level of the external leads, giving rise to a peak in i_D . We stress the fact that the time evolution is

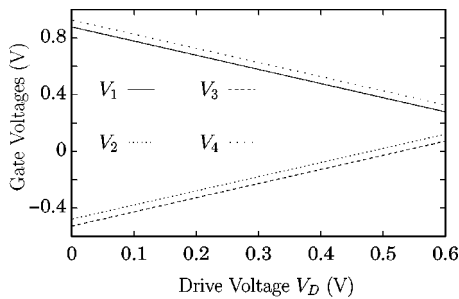


FIG. 3. Voltage ramps applied to the external gates in order to vary the chemical potentials of the dots. Using this setup, the chemical potentials of the two dots forming a pair are aligned with the Fermi energy levels of the external lead, allowing current to flow.

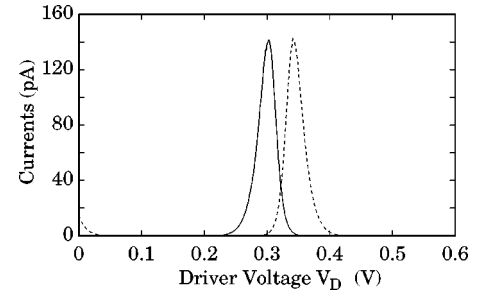


FIG. 4. Current peaks of i_U (solid line) and of i_D (dashed line) when only the upper and the lower pair of dots, respectively, are operated. The current peaks are well separated due to the shift we introduced between the upper and the lower voltage ramps.

assumed to be very slow, so that the behavior of the circuit can be considered quasistationary.

The upper pair of dots is operated in the same way. However, as shown in Fig. 3, we have introduced a shift between the upper and the lower ramps. In this way, as reported in Fig. 4, the current peaks of i_U and i_D that we obtain when only the upper and the lower pair of dots, respectively, are operated, are well separated. When the two pumps are operated at the same time, the current peaks show a *locking effect* due to the electrostatic interaction represented in Fig. 1 by the C_A capacitors, which is discussed in detail in Ref. 27. In some sense, the current i_U , which starts earlier than current i_D , *drives* the current i_D in the first part of the locking process, while in the second part i_D drives i_U . This locking effect of current peaks is reported in Fig. 5. We have investigated the shot noise of currents i_U and i_D in this regime, and our results are reported in Fig. 6. When the current i_U drives the current i_D , it exhibits the typical suppressed shot noise. Instead, current i_D , the driven one, presents a peculiar shot-noise enhancement. The maximum enhancement occurs when the difference between i_U and i_D reaches its largest value. Then shot noise for both currents approaches the Poissonian value, i.e., the Fano factor γ tends to 1. Full shot noise, i.e., $\gamma = 1$, is retrieved when i_U and i_D have about the same value and there are no more a driver and a driven current. Beyond this point, the roles of current i_U and i_D are exchanged, and i_U becomes the driving current while i_D becomes the driven one. The shot-noise behavior is also interchanged, as shown in Fig. 6.

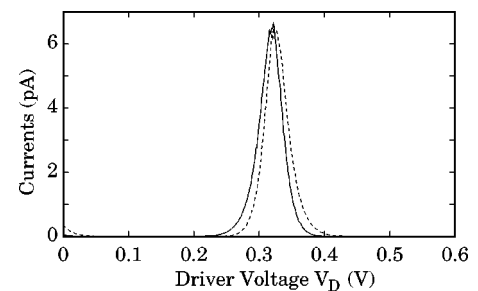


FIG. 5. Current peak of i_U (solid line) and of i_D (dashed line) when the upper and the lower pair of dots are operated at the same time. A locking effect (Ref. 27) due to electrostatic coupling between the two pairs of dots is shown.

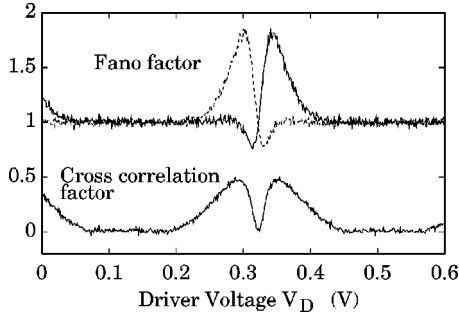


FIG. 6. The upper curves show Fano factor of currents i_U (solid line) and i_D (dashed line) when the two pairs of dots of the CMDD structure are operated at the same time, with the voltages shown in Fig. 3. Both Fano factors show a large enhancement with respect to the full shot level, and a typical suppression. The enhancement occurs when the electron transport is driven by the current in the other pump. In the driving regime, the Fano factor exhibits suppression. In the lower curve we have reported the cross correlation between the two currents. Where there is the maximal enhancement of shot noise, there is also the maximal correlation between the two currents.

We have also considered the cross-correlation factor between current i_U and i_D . In the lower curve of Fig. 6 we have reported the result of the simulation. Indeed, we find that there is a significant correlation between the two currents when the driver/driven mechanism is active. The curve is symmetric with respect to the point where the currents change their roles. In this point, as one can expect, there is no correlation at all.

IV. ANALYTICAL MODEL

We have also developed an analytical model valid in the zero-temperature limit. In this regime only few transitions are allowed, and the mechanism that leads to current transport is well understood. The formalism we use was proposed by Korotkov²⁰ for the optimization of the theoretical sensitivity of a single-electron transistor used as an electrometer.²⁸

The idea is based on a path-integral approach to random walk. The transport process is regarded as a path in the charge configuration space. A single charge configuration can be represented by the quadruplet indicating the amount of charge, in electron units, contained in each of the four quantum dots in the CMDD. In our case, we are interested only in configurations in which the number of electrons in each dot can take on only two values. Without loss of generality, we can assume that the two values are 0 and 1. We have represented the quadruplet with four circles and we have codified 0 with the white color and 1 with the black color (see Fig. 7).

A path can be divided into sequential jumps between charge configurations, with each jump characterized by a transition-rate probability. Let us refer to a single path as ξ . Then, for each path ξ , we can evaluate the probability of the path $P(\xi)$, the time it takes to go through this path $\tau(\xi)$ and the charge $e k(\xi)$ that flows through the voltage source during this path.

Once we have determined the main paths that form the

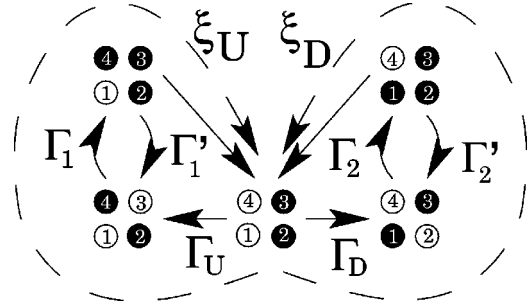


FIG. 7. Sketch of the two paths ξ_U and ξ_D that allow current to flow in the upper and in the lower pairs of dots, respectively, making up the CMDD.

transport process, we can evaluate, by performing the average on this ensemble of paths, the mean time of the process $\overline{\mathcal{T}} = \overline{\tau(\xi)}$, and the average charge that has flowed through the voltage sources $\overline{Q} = e \overline{k(\xi)}$. Using these quantities, we have the mean current $I = \overline{Q}/\overline{\mathcal{T}}$.

Following the definitions of the power-spectrum estimator given by Eq. (4) and by Eq. (5), we can obtain an expression for the Fano factor as a function of averages on the path ensemble,

$$\begin{aligned} \gamma &= \frac{1}{2eI} \frac{2}{\tau(\xi)} \left(\int_0^{\tau(\xi)} [i(t) - I] dt \right)^2 \\ &= \frac{1}{2eI} \frac{2}{\tau(\xi)} [ek(\xi) - I\tau(\xi)]^2 \\ &= \frac{1}{2eI} \frac{2}{\tau(\xi)} [e^2 k^2(\xi) - 2ek(\xi)\tau(\xi) + I^2 \tau^2(\xi)] \\ &= \frac{1}{\tau(\xi)} \left(\frac{\overline{\tau(\xi)}}{ek(\xi)} ek^2(\xi) - 2k(\xi)\tau(\xi) + \frac{ek(\xi)}{\tau(\xi)} \frac{\tau^2(\xi)}{e} \right) \\ &= \frac{\overline{k^2(\xi)}}{k(\xi)} - 2 \frac{\overline{k(\xi)\tau(\xi)}}{\tau(\xi)} + k(\xi) \frac{\overline{\tau^2(\xi)}}{\tau(\xi)^2}. \end{aligned} \quad (10)$$

Let us return to our model. By a direct inspection of tunneling rates as the temperature tends to zero, we have been able to extract the main transitions giving rise to current flow in the device. We start from the configuration with the two excess electrons in the right column (see Fig. 7). From this configuration we have sketched the two possible paths in the charge configuration space. The first path, which we indicate with ξ_U , allows current to flow in the upper pair of dots, while the second path, which we indicate with ξ_D , allows current to flow in the lower pair of dots. The probability to follow path ξ_U is $P(\xi_U) = \Gamma_U / (\Gamma_U + \Gamma_D)$ and that to follow path ξ_D is $P(\xi_D) = \Gamma_D / (\Gamma_U + \Gamma_D)$, where Γ_U and Γ_D are the probabilities per unit time of leaving the starting configuration as reported in Fig. 7.

At low temperature, the transition rates Γ_1 , Γ'_1 and Γ_2 , Γ'_2 (the corresponding transitions are indicated in Fig. 7) are

much smaller than all the other transition rates. This implies that flow through path ξ_U and ξ_D obeys Poissonian statistics with mean time $\tau(\xi_U)=1/(\Gamma_1+\Gamma'_1)$ and $\tau(\xi_D)=1/(\Gamma_2+\Gamma'_2)$ and with mean square time $\tau^2(\xi_U)=2/(\Gamma_1+\Gamma'_1)^2$ and $\tau^2(\xi_D)=2/(\Gamma_2+\Gamma'_2)^2$.

Using these expressions we can evaluate the mean time of the process, as required by Eq. (10)

$$\begin{aligned}\bar{\tau} &= P(\xi_U)\tau(\xi_U)+P(\xi_D)\tau(\xi_D) \\ &= \frac{\Gamma_U}{\Gamma_U+\Gamma_D} \frac{1}{\Gamma_1+\Gamma'_1} + \frac{\Gamma_D}{\Gamma_U+\Gamma_D} \frac{1}{\Gamma_2+\Gamma'_2},\end{aligned}\quad (11)$$

and the mean square time

$$\bar{\tau}^2 = \frac{\Gamma_U}{\Gamma_U+\Gamma_D} \frac{2}{(\Gamma_1+\Gamma'_1)^2} + \frac{\Gamma_D}{\Gamma_U+\Gamma_D} \frac{2}{(\Gamma_2+\Gamma'_2)^2}.\quad (12)$$

As far as the charge that flows through the voltage sources is concerned, we notice that we can distinguish between path ξ_U for which there is no charge flowing in the lower pair of dots, and ξ_D for which there is no charge flowing in the upper pair of dots. We have that current i_U (i_D) is not zero when the system follows path ξ_U (ξ_D), and only in this case it makes sense to evaluate the Fano factor (10). Thus, we have two different Fano factors, γ_U for the upper current, and γ_D for the lower one. Let us use the subscripts U and D for quantities referring to the upper and lower pair of dots, respectively. We have

$$\bar{k}_U = \frac{\Gamma_U}{\Gamma_U+\Gamma_D} \frac{\Gamma_1}{\Gamma_1+\Gamma'_1},\quad (13)$$

$$\bar{k}_D = \frac{\Gamma_D}{\Gamma_U+\Gamma_D} \frac{\Gamma_2}{\Gamma_2+\Gamma'_2},\quad (14)$$

and

$$\overline{k\tau}_U = \frac{\Gamma_U}{\Gamma_U+\Gamma_D} \frac{\Gamma_1}{\Gamma_1+\Gamma'_1} \frac{1}{\Gamma_1+\Gamma'_1},\quad (15)$$

$$\overline{k\tau}_D = \frac{\Gamma_D}{\Gamma_U+\Gamma_D} \frac{\Gamma_2}{\Gamma_2+\Gamma'_2} \frac{1}{\Gamma_2+\Gamma'_2},\quad (16)$$

and $\overline{k_U^2}=k_U$, and $\overline{k_D^2}=k_D$. If we substitute the above values in Eq. (10), we find the following expressions for the Fano factor of the upper and lower currents:

$$\gamma_U = 1 + \frac{2\Gamma_1}{\Gamma_1+\Gamma'_1} \epsilon \frac{1-\delta}{(\delta+\epsilon)^2},\quad (17)$$

$$\gamma_D = 1 + \frac{2\Gamma_2}{\Gamma_2+\Gamma'_2} \epsilon \delta \frac{\delta-1}{(\delta+\epsilon)^2},\quad (18)$$

where $\delta=(\Gamma_2+\Gamma'_2)/(\Gamma_1+\Gamma'_1)$ and $\epsilon=\Gamma_D/\Gamma_U$. In Fig. 8 we compare the values obtained from the analytical expressions

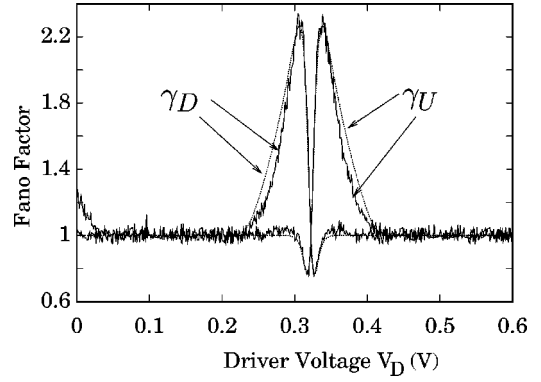


FIG. 8. Comparison between the Fano factor computed with the analytical expression (dotted line) and the result of a Monte Carlo simulation at the temperature of 10 K (solid line).

(17) and (18) with those from the Monte Carlo simulations, at a temperature of 10 K. There is good quantitative agreement between the two curves.

We have also investigated the behavior of the maximum Fano factor as a function of the ratio $r=R_U/R_D$ of the tunneling resistances. When, for instance, the voltage configuration is such that the lower current exhibits a maximum Fano factor, we have that $\Gamma_1, \Gamma'_1 \ll \Gamma_2, \Gamma'_2$, and, therefore, the condition $\delta \gg \epsilon$. Thus, Eq. (17) becomes

$$\gamma_D - 1|_{\max} \approx 2 \frac{\Gamma_2}{\Gamma_2+\Gamma'_2} \frac{\Gamma_D}{\Gamma_U}.\quad (19)$$

According to the orthodox theory, [Eq. (1)], the transition rate is proportional to the inverse of the tunneling resistance, and the free-energy variation between different configurations does not depend on the tunneling resistance, but only on the capacitance and voltage values. Therefore, at given capacitance and voltage values, we have that $\gamma_D - 1|_{\max} = \Lambda r$, with all the dependence on capacitances and voltages in Λ . Taking $r=1$ as a reference value, we obtain

$$\frac{\gamma_D - 1}{\gamma_D^0 - 1}|_{\max} = r,\quad (20)$$

where $\gamma_D^0 = \gamma_D(r=1)$. In Fig. 9(a) we have plotted the Fano factor for different values of the ratio r . In Fig. 9(b) the maximum Fano factor is plotted as a function of the ratio r and is shown to be in good agreement with Eq. (20) (solid line). We want to point out that (20) is valid in the zero-temperature limit, while the Fano factors in Fig. 9(a) are computed at $T=10$ K, thus thermal fluctuations are present.

V. CONCLUSIONS

In this paper we have investigated the shot-noise behavior of a system of coupled quantum dots. We have carried out our analysis by means of a Monte Carlo algorithm based on the orthodox theory of SET's, and of analytical methods.

We have started our numerical analysis evaluating shot noise in a single-electron pump, where we only have sup-

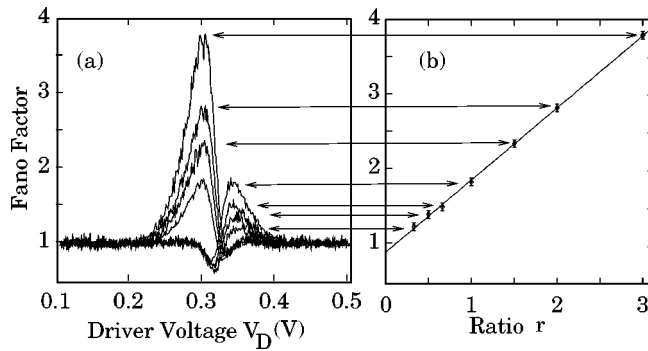


FIG. 9. In Fig. 9(a) we have different Fano factor with different ratio between the upper and lower tunneling resistance. Changing the ratio we change also the value of the maximum of the Fano factor. In Fig. 9(b) such a maximum is reported as a function of the ratio, in agreement with the linear dependence of Eq. (20).

pression of shot noise, and we succeeded in reproducing the honeycomb structure, well known in the current domain, using the Fano factor. At the triple points of the honeycomb structure, shot-noise suppression is maximum (1/3 of the full shot level) in agreement with the known literature.

Then we have analyzed shot noise in a CMDD structure operated so that the upper and the lower pairs of dots, making up the CMDD, were brought out of the Coulomb blockade at the same time. In this case we have found a significant deviation from full shot noise and a very peculiar pattern of the Fano factor. We have obtained both a suppression and an enhancement of shot noise: while the suppression is a typical behavior of SET systems, there are few examples of noise enhancement. This enhancement is due to the correlation between the upper and the lower currents of a CMDD, as a consequence of Coulomb interaction.

At low temperature, the transport is only due to few transitions. In this limit we have been able to carry out an analytical investigation of the Fano factor behavior, and our results are in good agreement with the Monte Carlo simulations. With the analytical approach we have also shown that the maximum value of the Fano factor depends on the ratio between the upper and lower resistance values.

Several single-electron tunneling systems may exhibit noise properties similar to those we have presented in this paper. While suppression of shot noise is straightforward to obtain, when electrostatic interaction regulates successive tunneling events through a junction, we believe that the major result of the present paper is the demonstration that shot noise can be enhanced due to a combined effect of Coulomb interaction and system topology. The system considered in this paper is one of the simplest single-electron circuits exhibiting such properties, and in this sense has represented an excellent testbed for our analytical and numerical tools for the investigation of noise. The noise behavior described in this paper could be measured, for example, in experiments on the silicon-on-insulator structures considered in Ref. 27. In that case, the equivalent capacitance matrix of the system would include additional terms due to coupling between dots and gates, and quantum confinement within a dot would play a role in the free energy of the system. Simulations on that system have shown us that the enhancement and suppression of shot noise would be still significant and well detectable.

Let us conclude by pointing out that in SET systems noise plays a much more important role than in standard electronic circuits. While in the latter noise is just a small fluctuation, often negligible with respect to the average value, in the former the current consists of well separated pulses, thereby requiring, for a meaningful design, a full comprehension of the stochastic nature of the process.

*Electronic address: gatto@sns.it

¹W. Schottky, *Ann. Phys. (Leipzig)* **57**, 541 (1918).

²Y. Blanter and M. Büttiker, *Phys. Rep.* **336**, 1 (2000).

³S. Hershfield, J. H. Davies, P. Hyldgaard, C. J. Stanton, and J. W. Wilkins, *Phys. Rev. B* **47**, 1967 (1993).

⁴H. Birk, M. J. M. de Jong, and C. Schonenberger, *Phys. Rev. Lett.* **75**, 1610 (1995).

⁵Z. Wang, M. Iwanaga, and T. Miyoshi, *Jpn. J. Appl. Phys., Part 1* **37**, 5894 (1998).

⁶S. Sasaki, K. Tsubaki, S. Tarucha, A. Fujiwara, and Y. Takahashi, *Solid State Electronics* **42**, 1429 (1998).

⁷K. A. Matsuoka and K. K. Likharev, *Phys. Rev. B* **57**, 15 613 (1998).

⁸A. N. Korotkov and K. K. Likharev, *Phys. Rev. B* **61**, 15 975 (1999).

⁹Y. A. Kinkhabwala and A. N. Korotkov, *Phys. Rev. B* **62**, R7727 (2000).

¹⁰E. R. Brown, *IEEE Trans. Electron Devices* **39**, 2686 (1992).

¹¹M. M. Jahan and A. F. M. Anwar, *Solid-State Electron.* **38**, 429 (1995).

¹²V. V. Kuznetsov, E. E. Mendez, J. D. Bruno, and J. T. Pham, *Phys. Rev. B* **58**, R10 159 (1998).

¹³G. Iannaccone, M. Macucci, and B. Pellegrini, *Phys. Rev. B* **55**, 4539 (1997).

¹⁴G. Iannaccone, G. Lombardi, M. Macucci, and B. Pellegrini, *Phys. Rev. Lett.* **80**, 1054 (1998).

¹⁵Y. M. Blanter and M. Büttiker, *Phys. Rev. B* **59**, 10 217 (1999).

¹⁶A. Reklaitis and L. Reggiani, *Phys. Rev. B* **62**, 16 773 (2000).

¹⁷V. Y. Aleshkin, L. Reggiani, and A. Reklaitis, *Phys. Rev. B* **63**, 085302 (2001).

¹⁸H. Pothier, P. Lafarge, P. F. Orfila, C. Urbina, D. Esteve, and M. H. Devoret, *Physica B* **169**, 573 (1991).

¹⁹H. Pothier, P. Lafarge, C. Urbina, D. Esteve, and M. H. Devoret, *Europhys. Lett.* **17**, 249 (1992).

²⁰A. N. Korotkov, *Phys. Rev. B* **49**, 10 381 (1994).

²¹N. S. Bakhvalov, G. S. Kazacha, K. K. Likharev, and S. I. Serdyukova, *Zh. Eksp. Teor. Fiz.* **95**, 1010 (1989) [*Sov. Phys. JETP* **68**, 581 (1989)].

²²C. S. Lent, P. D. Tougaw, and W. Porod, *Appl. Phys. Lett.* **62**, 714 (1993).

²³M. Governale, M. Macucci, G. Iannaccone, C. Ungarelli, and J. Martorell, *J. Appl. Phys.* **85**, 2062 (1999).

- ²⁴L. Bonci, G. Iannaccone, and M. Macucci, *J. Appl. Phys.* **89**, 6435 (2001).
- ²⁵D. Esteve, in *Single Charge Tunneling Coulomb Blockade Phenomena in Nanostructures*, edited by H. Grabert and M. H. Devoret (Plenum Press, New York, 1992), pp. 109–137.
- ²⁶M. Eto, *J. Phys. Soc. Jpn.* **65**, 1523 (1996).
- ²⁷M. Macucci, M. Gattobigio, and G. Iannaccone, *J. Appl. Phys.* **90**, 6428 (2001).
- ²⁸A. N. Korotkov, D. V. Averin, K. K. Likharev, and S. A. Vasenko, in *Single-Electron Tunneling and Mesoscopic Devices*, edited by H. Koch and H. Lübbig (Springer-Verlag, Berlin, 1992), p. 45.